Development and characterization of a free fatty acid receptor 2 (FFA2) fluorescent tracer

Anders Højgaard Hansen[†,§], Eugenia Sergeev[‡,§], Sunil K. Pandey[†], Brian D. Hudson[‡], Elisabeth Christiansen[†], Graeme Milligan[‡] and Trond Ulven[†]*

[†]Department of Physics, Chemistry and Pharmacy, University of Southern Denmark, Campusvej 55, DK-5230 Odense M, Denmark

[‡]Centre for Translational Pharmacology, Institute of Molecular, Cell and Systems Biology, College of Medical, Veterinary and Life Sciences, University of Glasgow, Glasgow G12 8QQ, Scotland, United Kingdom

ABSTRACT

The free fatty acid receptor 2 (FFA2/GPR43) is considered a potential target for treatment of metabolic and inflammatory diseases. Here we describe the development of the first fluorescent tracer for FFA2 intended as a tool for assessment of thermodynamic and kinetic binding parameters of unlabeled ligands. Starting with a known azetidine FFA2 antagonist, we used a carboxylic acid moiety known not to be critical for receptor interaction for the attachment of a nitrobenzoxadiazole (NBD) fluorophore. This led to the development of **4** (TUG-1609), a potent fluorescent tracer for FFA2 with good spectroscopic properties, high affinity as determined by saturation and kinetic binding experiments, and high specific to non-specific binding to NanoLuciferase (Nluc) tagged FFA2. A BRET-based competition binding assay with **4** was established and used to determine binding constants and kinetics of unlabeled ligands.

INTRODUCTION

The free fatty acid receptor 2 (FFA2, also known as GPR43) is a 7-transmembrane receptor activated by short-chain fatty acids (SCFAs) produced endogenously during colonic fermentation of dietary fiber by the gut microbiota.[1-4] The receptor is expressed in various cell types such as adipocytes and pancreatic β-cells.[5,6] FFA2 is also expressed in immune cells, including neutrophils, eosinophils, B lymphocytes, and peripheral blood mononuclear cells, and has been shown to mediate SCFA-promoted chemotaxis in neutrophils.[7-10] In recent years FFA2 has attracted much attention as a possible target for treatment of obesity,[11] inflammation,[8,12,13] and metabolic diseases.[4,14] It has however frequently been unclear if the preferred mode of action was agonism or antagonism.[2] It has been shown that the loss of FFA2 and the related SCFA receptor FFA3 (GPR41) leads to increased insulin secretion and improved glucose tolerance, indicating a therapeutic potential of antagonists against metabolic diseases.[6] The role of the receptor in chemotaxis of neutrophils has also suggested anti-inflammatory potential of antagonists. For example, the FFA2 antagonist GLPG0974 (**1**, Chart 1) has been demonstrated to inhibit human neutrophil recruitment *in vitro* and *in vivo*, suggesting that the compound could represent a potential therapeutic for treatment of inflammatory diseases.[12,15] Clinical trials with **1** for treatment of ulcerative colitis indeed showed decreased neutrophil infiltration although no significant improvement of symptoms was observed in the patients.[16] To fully assess the therapeutic potential of FFA2, high quality tool compounds are needed for further investigations of FFA2 pharmacology and function.

Fluorescent tracer molecules have been established as useful tools for real-time monitoring of receptor-ligand interactions and offer several advantages over conventional radioactive

tracers.[17,18] The small, green-emitting fluorophore 4-amino-7-nitrobenzoxadiazole (NBD) has previously been employed for labeling small molecules and proteins and has been applied in competition binding assays and for imaging of living cells.[19,20] Its absorption and emission maxima, around 470 nm and 530 nm, respectively, are above the cellular autofluorescence range and therefore make NBD a useful probe for *in vitro* biological studies.[21] The fluorescence of NBD is almost completely quenched in polar and protic solvents, whereas high fluorescence activity is preserved in non-polar environments, which can amplify signal to noise ratio for the bound NBD.[22] Bioluminescence resonance energy transfer (BRET) interaction between a tagged receptor and a fluorescent ligand is useful for real-time interaction monitoring, also between GPCRs and small molecules.[23] We have recently taken advantage of the properties of NBD by developing two free fatty acid receptor 1 (FFA1) fluorescent tracers as well as a BRET competition binding assay to NanoLuciferace (NLuc) tagged FFA1 and demonstrated its usefulness for investigating the binding of natural and synthetic ligands to the FFA1 receptor.[18] Recognizing the need for a similar fluorescent tracer and assay for FFA2, we aimed to follow an equivalent strategy for this receptor. We here report on the design, synthesis and characterization of the first fluorescent tracer for FFA2 and the use of the tracer in a BRET competition binding assay. The carboxylic acid chain of **1** was originally introduced to tackle ADME issues in the compound series.[12] Although the carboxylate contributes somewhat to potency of the compound and has been demonstrated to depend on the presence of at least one of the two orthosteric arginine residues, the group is not required for the activity of the compound.[24] The closely related azetidine analogue **2** as well as its methyl ester (**3**) are also efficient FFA2 antagonists.[12,24] As the carboxylic acid group appeared to be dispensable for the affinity of the

compounds, we decided to explore this group as attachment point for an NBD fluorophore in the design of the proposed FFA2 fluorescent tracer **4** (Chart 1).

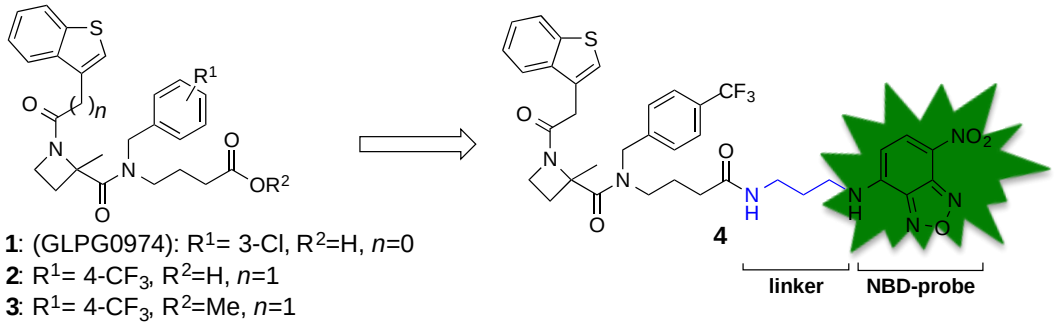

Chart 1. Design strategy for an antagonist-based FFA2 fluorescent tracer.

RESULTS AND DISCUSSION

Synthesis

The fluorescent tracer **4** was synthesized in 13 steps from commercial starting materials. Azetidine **5** was synthesized according to the procedures described by Pizzonero and co-workers (Scheme 1).[12] Benzothiene-3-acetic acid **6** was activated with bis(2-oxo-3-oxazolidinyl)phosphinic chloride (BOP-Cl) and coupled with **5** to give **3**. Methyl ester **3** was hydrolyzed to carboxylic acid **2**, activated using BOP-Cl and coupled to mono-Boc-protected 1,3-diaminopropane to give **7**. Boc-deprotection afforded the crude amine, which was reacted directly with NBD-Cl in a nucleophilic aromatic substitution to give the fluorescent **4** in 47% yield after purification by preparative HPLC.[18]

Scheme 1. Synthesis of **4**.[a]

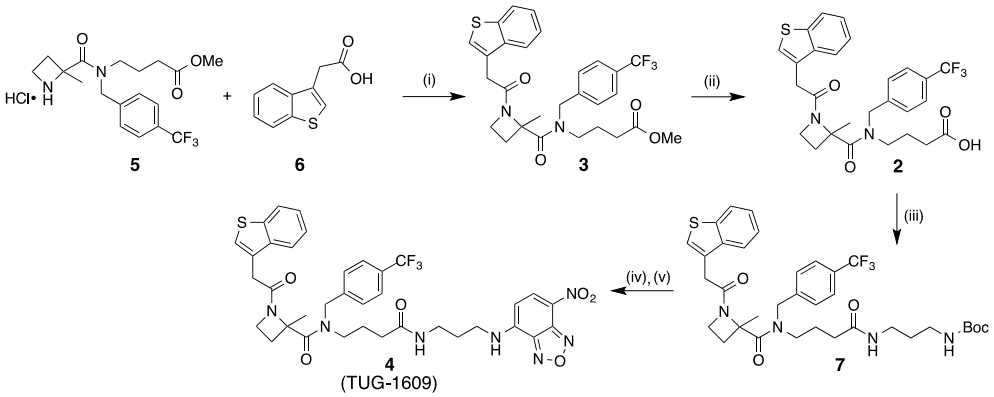

[a]Reagents and conditions: (i) Et_3N, BOP-Cl, DCM, 80 °C, 25 h, 40%; (ii) LiOH, THF, water, rt, 96%; (iii) a): Et_3N, BOP-Cl, DCM, 50°C, 3 h; b): Et_3N, *tert*-butyl (3-aminopropyl)carbamate, 30 min at 50 °C, then rt overnight, 46%; (iv) TFA, DCM, rt; (v) NBD-Cl, $NaHCO_3$, MeOH, 50 °C, 4 h, 38% over 2 steps.

Characterization of Fluorescent Properties

Absorbance and fluorescence spectra of **4** were recorded in PBS and in *n*-octanol, with the latter solvent emulating the environment of a predominately hydrophobic receptor binding site or membrane.[25] A shift of 30 nm was observed when comparing the maximum absorption of **4** in *n*-octanol (λ_{max} = 462 nm) with that in PBS buffer (λ_{max} = 492 nm, spectrum not shown). The extinction coefficient (ε) of **4** at its maximum excitation wavelength was determined ($\varepsilon_{462\ nm}$ = 12,550 M^{-1} cm^{-1}) from absorbance spectra recorded in *n*-octanol at increasing concentrations of **4** (Table 1). Fluorescent tracer **4** exhibits maximum emission at 525 nm with a Stokes shift of 63 nm and a quantum yield (Φ) of 0.62 in *n*-octanol (Table 1 and Figure 2A), whereas the fluorescence was almost absent in PBS (Figure 2B). Overall, **4** demonstrated properties comparable to the values observed for the recently reported NBD-based FFA1 tracers.[18]

Table 1. Fluorescent properties of **4**.

n-Octanol					PBS buffer (pH 7.4)	
λ_{ex} [nm]	λ_{em} [nm]	SS [nm]	$\varepsilon_{462\ nm}$ [$M^{-1}\ cm^{-1}$]	Φ	λ_{ex} [nm]	λ_{em} [nm]
462	525	63	12,550 ± 276	0.62	492	557

[a]SS, Stokes shift; Φ, quantum yield.

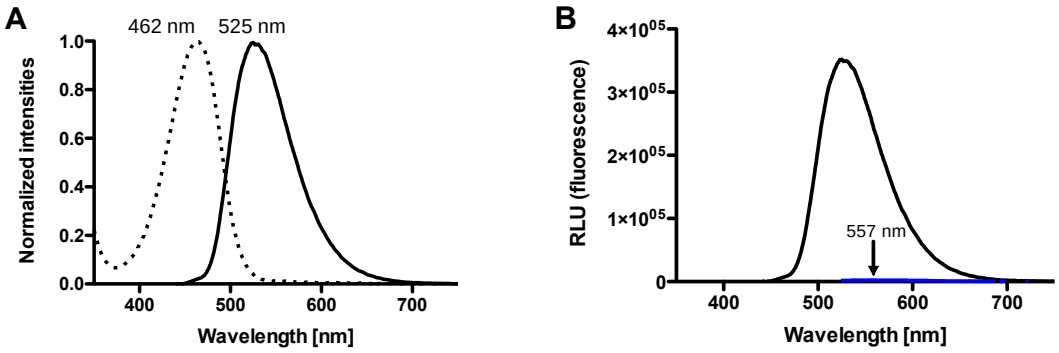

Figure 2. Absorbance and fluorescent properties of **4**. A) Normalized exitation (dotted line) and emission (solid line) spectra in *n*-octanol. B) Effect of solvent on fluorescence activity of **4** in *n*-octanol (black curve) and PBS buffer (blue curve).

Functional Characterization of 4 on FFA2

Tracer **4** was found to act as an antagonist of propionate (C3)-mediated elevation of inositol monophosphate (IP1) levels in Flp-In™ T-REx™ 293 cells induced to express a form of human FFA2 that had enhanced Yellow Fluorescent Protein linked in frame to the intracellular C-terminal tail of the receptor (hFFA2-eYFP) (Figure 3A). The ability of **4** to inhibit the effects of an EC_{80} concentration of C3 was similar to that of the related clinically tested FFA2 antagonist **1** and analogue **2** (Figure 3A, Table 2). Furthermore, in membrane preparations derived from these

cells, increasing concentrations of **4** were able to prevent specific binding of [^{3}H]-**1** to the hFFA2-eYFP construct with affinity akin to that of unlabeled **1** (pK_i = 7.76 ± 0.11) and **2** (Figure 3B, Table 2).

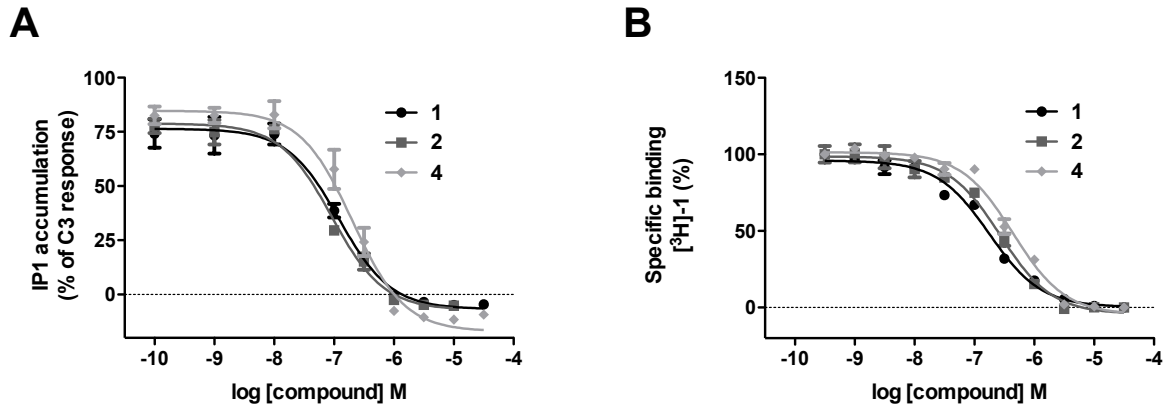

Figure 3. (A) Functional characterization of **4** against **1** and **2** in IP1 accumulation assay. (B) Displacement of [^{3}H]-**1** using **1**, **2** and **4**.

Table 2. Characterization of antagonist properties and affinities of unlabeled carboxylic acid **1**, methyl ester **2** and fluorescent tracer **4** as antagonist in functional IP1 and radioligand displacement assays.

Cmpd	pIC_{50} (IP1)[a]	pK_i (Displacement)[b]
1	6.94 ± 0.04	7.76 ± 0.11
2	7.08 ± 0.05	7.64 ± 0.08
4	6.57 ± 0.10	7.31 ± 0.06

[a]The ability of **4** to inhibit IP1 accumulation at EC_{80} concentration of propionate. [b]K_i was determined in a [^{3}H]-**1** displacement assays.

Characterization of 4 as an FFA2 Tracer Molecule

A saturation binding experiment was performed by adding varying concentrations of **4** to membrane preparations generated from Flp-In™ T-REx™ 293 cells induced to express a form of human FFA2 that has an NLuc enzyme incorporated into the extracellular N-terminal domain of the receptor. This allowed BRET (Figure 4A) between NLuc and the NBD domain of bound **4**. Subtraction of signal obtained when the same concentrations of **4** were co-incubated with 50 μM **1** was used to define non-specific binding of **4** (Figure 4A) and to generate a monophasic binding curve with an estimated K_d for **4** of 65.1 ± 1.8 nM (Figure 4B). Following addition of 100 nM **4** to membrane preparations and waiting 2 hours to allow binding to reach equilibrium, wash-out of unbound **4** allowed the dissociation of **4** to be monitored under conditions of infinite dilution by the reduction of specific BRET signal over time (Figure 4C). Time courses of development of specific BRET signals following addition of different concentrations of **4** showed the estimated ligand association rate to increase with ligand concentration as predicted by mass action (Figure 4D). These experiments allowed the determination of a dissociation constant k_{off} of 0.0249 ± 0.0009 min^{-1} and an association constant k_{on} of 368,000 ± 29300 M^{-1} min^{-1} for tracer **4**. Using these constants to independently calculate the affinity of **4** yielded a K_d of 67.7 nM, a value very close to that obtained from the saturation binding experiment.

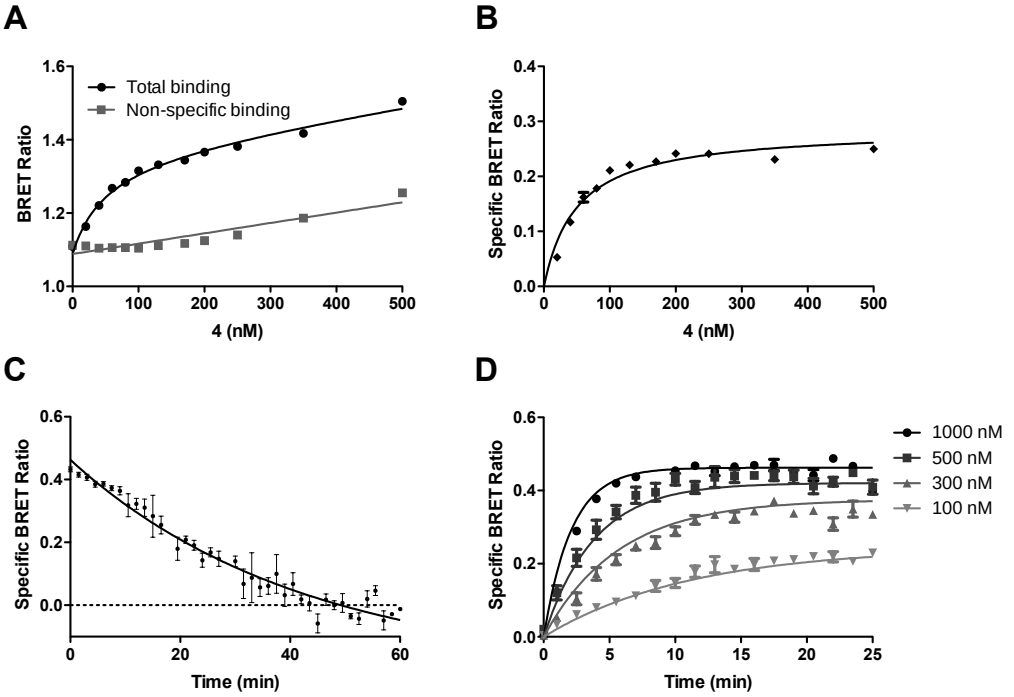

Figure 4. (A) BRET-based saturation binding experiment of tracer **4** bound to NLuc tagged FFA2 (Total binding); BRET between **4** and NLuc tagged FFA2 recorded using non-fluorescent **1** at high concentration (10 μM) (non-specific binding). (B) Monophasic binding curve for **4** obtained by subtracting total binding from non-specific binding of **4**. (C) Dissociation of **4** monitored under conditions of infinite dilution. (D) Time courses measuring the association of **4** to NLuc tagged FFA2 at varying concentrations of **4**.

To compare the usefulness of **4** with that of the radiolabeled FFA2 antagonist [^{3}H]-**1**, we employed the BRET signal produced by **4** bound specifically to NLuc tagged FFA2 in the presence of varying concentrations of either **1** or the FFA2 antagonist CATPB (**8)** as a means to concomitantly measure both 'on' and 'off' rates of these unlabeled ligands (Table 3). Antagonist **8** is structurally different from **1** but is known to bind to the same site at the FFA2 receptor.[24,26] Previous studies using [^{3}H]-**1** indicated that although these two compounds have similar affinity

at human FFA2, **8** is relatively 'fast on-fast off' whilst **1** displays both slower association and slower dissociation kinetics.[24] These features were reproduced and confirmed when employing **4** in such binding kinetic analyses (Figure 5). The rate constants corresponded to dissociation constants of 46.9 nM and 18.9 nM for **1** (Figure 5A) and **8** (Figure 5B), respectively (Table 3).

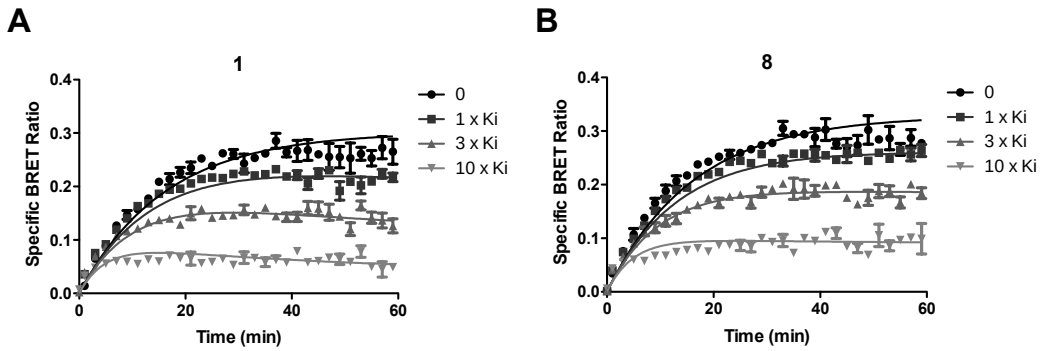

Figure 5. Application of **4** in binding kinetic analyses of unlabeled ligands; (A) **1**, (B) **8**.

Table 3. Kinetic properties for fluorescent tracer **4** and unlabeled ligands **1** and **8**.

Cmpd	k_{off} (min^{-1})	k_{on} (M^{-1} min^{-1})	K_d (nM)
4[a]	0.0249 ± 0.0009	368,000 ± 29300	65.1
1[b]	0.0099 ± 0.0014	211,000 ± 4780	46.9
8[b]	0.0205 ± 0.0010	1,083,000 ± 59800	18.9

[a]Rate constants and dissociation constant of **4** determined in BRET-based saturation binding assay. [b]Rate constant and dissociation constants for unlabeled ligands **1** and **8** determined using tracer **4** in BRET-based competition binding assay.

Importantly, when varying concentrations of **4** were co-added with a range of concentrations of **1**, analysis of the binding of **4**, as reported by the specific BRET signal, was consistent with competition between the ligands to bind to the receptor (Figure 6A). Higher concentrations of **4**

required increasing concentrations of **1** to compete for the receptor binding site (Figure 6A, Table 4). Equivalent conclusions were reached for **8** (Figure 6B) and provided an estimated affinity for human FFA2 of 14.5 nM, almost identical to the value determined previously when employing [^{3}H]-**1**.[24] Notably, affinity values for **1** and **8** determined using **4** in competition binding experiments (Table 4) were found to be internally consistent with dissociation constants obtained when using **4** in binding kinetic analyses (Table 3). To be useful as a ligand with which to screen novel chemical ligands for affinity at human FFA2, it is important that employing **4** should result in ligand structure activity relationships (SAR) as anticipated from other studies. It is known that replacement of the carboxylate moiety of **8** by methyl ester (**9**) reduces affinity at hFFA2 by more than 10 fold.[24] Herein, using **4** this expectation was again fulfilled (Figure 6C) with **9** displaying 23.6 fold lower affinity for human FFA2, when compared to **8**.

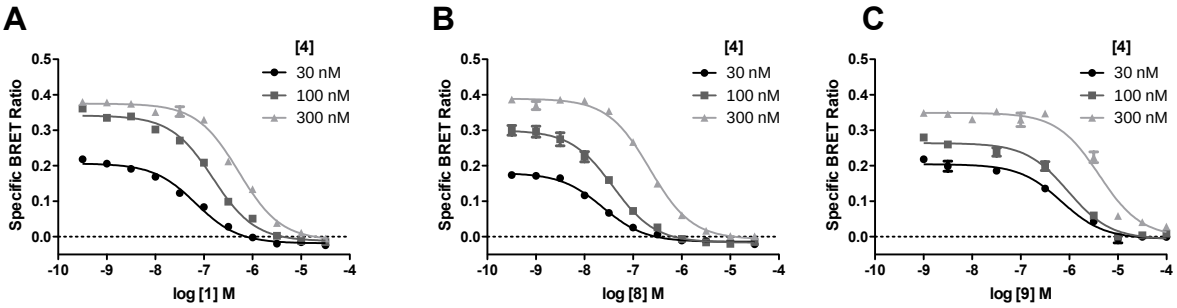

Figure 6. Application of **4** in competition binding experiments of unlabeled ligands (A) **1**, (B) **8**, (C) **9**.

Table 4. Competition binding affinities of selected FFA2 antagonists.

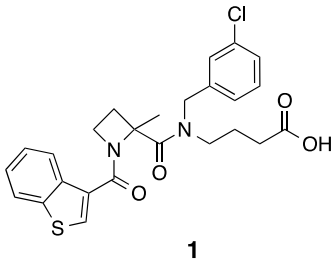

1

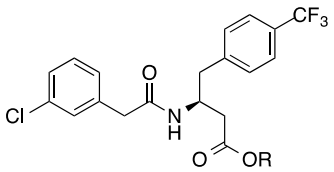

8 (CATPB): R=H
9: R=Me

		1	**8**	**9**
Affinity	pK_i	7.16 ± 0.06	7.84 ± 0.04	6.42 ± 0.03
	(nM)	69.2	14.5	380

CONCLUSION

By taking advantage of SAR information on known antagonists for FFA2, the fluorescent tracer molecule **4** was developed. Tracer **4** contains an NBD fluorescent probe and exhibits desirable spectroscopic properties, including a Stokes shift of 63 nm, low fluorescence activity in aqueous solution, and a high quantum yield in non-polar environments. Using an NLuc construct built into the extracellular N-terminal domain of the FFA2 receptor and BRET-based binding experiments, tracer **4** was found to exhibit a K_d of 65 nM and low non-specific binding. The BRET binding assay with **4** was further applied to determine thermodynamic and kinetic binding parameters of unlabeled FFA2 ligands, resulting in values comparable to those obtained previously using a radiolabeled ligand. Compound **4** is the first fluorescent tracer for FFA2 and is expected to be useful tool for further studies of the receptor as well as for characterization of FFA2 ligands.

EXPERIMENTAL SECTION

Synthesis

Commercial staring materials and solvents were used without further purification, unless otherwise stated. THF was freshly distilled from sodium/benzophenone, and MeOH and DCM were dried over 3 Å sieves. TLC was performed on TLC Silicage 60 F254 plates and visualized at 254 or 365 nm or by staining with ninhydrin or $KMnO_4$ stains. Purification by flash chromatography was carried out using silica gel 60 (0.040-0.063 mm, Merck). ^1H and ^{13}C NMR spectra were recorded at 400 and 101 MHz, respectively, on Bruker Avance III 400 at 300 K. Rotamer peaks have been assigned by asterisk (*). Purity was determined by HPLC and confirmed by inspection of NMR spectra (^1H and ^{13}C NMR). HPLC analysis was performed using a Gemini C18 column (5 μm, 4.6x150 mm); flow: 1 mL/min; 10% MeCN in water (0-1 min), 10-100% MeCN in water (1-10 min), 100% MeCN (11-15 min), with both solvents containing 0.1% HCOOH as modifier; UV detection at 254 nm. HPLC purification was performed by using a Phenomenex Luna C18 column (5 μm, 250×21.20 mm) with gradient elution of MeCN and water, with both solvents containing 0.1% HCOOH as modifier. High-resolution mass spectra (HRMS) were obtained on a Bruker micrOTOF-Q II (ESI).

Compounds **1**, **8** and **9** were synthesized according to published procedures.[12,27]

Methyl 4-(1-(2-(benzo[*b*]thiophen-3-yl)acetyl)-2-methyl-*N*-(4-(trifluoromethyl)benzyl)-azetidine-2-carboxamido)butanoate (3).

In a dry microwave vial carboxylic acid **6** (57.4 mg, 0.30 mmol) and amine **5** (93.4 mg, 0.23 mmol) were suspended in dry DCM (0.45 mL). To the stirred suspension were added Et_3N (175 μL, 1.26 mmol) and BOP-Cl (88.5 mg, 0.348 mmol), and the vial was heated at 80 °C for 25 h. The reaction was cooled to rt, vented, water was added, and the mixture extracted with DCM

(x5). The extract was dried over Na_2SO_4 and concentrated *in vacuo*. The product was obtained after flash chromatography (EtOAc:PE 4:1 → 100% EtOAc) as a pale yellow sticky oil (50.2 mg, 40%): R_f = 0.26 (EtOAc); ^{1}H NMR (400 MHz, $CDCl_3$) δ 7.95 – 7.53 (m, 4H), 7.50 – 7.12 (m, 5H), 4.94 – 4.26 (m, 2H), 4.10 – 2.96 (m, 6H), 3.66* (s, 3H), 3.63 (s, 3H), 2.63 – 2.46 (m, 1H), 2.43 – 2.14 (m, 3H), 2.00 – 1.71 (m, 5H); ^{13}C NMR (101 MHz, $CDCl_3$) δ 172.6, 172.0, 169.7, 141.4, 140.3, 139.3, 138.8, 130.1, 128.0, 126.9, 126.3, 125.8, 124.5, 124.3, 124.1, 124.0, 123.8, 122.9, 122.8, 122.1, 121.8, 71.0, 51.9, 51.8, 46.7, 46.3, 43.1, 34.4, 33.7, 31.3, 30.7, 29.4, 29.1, 23.8, 23.1; ESI-HRMS calcd for $C_{28}H_{29}F_3N_2NaO_4S$ ($M + Na^+$) 569.1692, found 569.1714.

4-(1-(2-(Benzo[*b*]thiophen-3-yl)acetyl)-2-methyl-*N*-(4-(trifluoromethyl)benzyl)azetidine-2-carboxamido)butanoic acid (2).

Compound **3** (50 mg, 91 μmol) dissolved in THF (1 mL) was added 0.6 M aqueous LiOH (0.45 mL) and stirred for 3.5 h at rt, whereafter the reaction mixture was acidified with 1 M HCl until pH 2-3 and extracted with EtOAc (x3). The extract was washed with brine, dried over Na_2SO_4, and concentrated *in vacuo* to give the desired product as a sticky oil (46.9 mg, 96%); ^{1}H NMR (400 MHz, $CDCl_3$) δ 7.93 – 7.51 (m, 4H), 7.49 – 7.13 (m, 5H), 4.93 – 4.26 (m, 2H), 4.09 – 2.95 (m, 6H), 2.61 – 2.43 (m, 1H), 2.40 – 2.12 (m, 3H), 2.00 – 1.70 (m, 5H); ^{13}C NMR (101 MHz, $CDCl_3$) δ 172.6, 172.6, 170.2, 140.3, 140.3, 139.3, 138.8, 130.1, 129.9, 128.0, 127.0, 125.8, 124.6, 124.3, 124.1, 124.0, 122.9, 122.8, 122.2, 122.0, 121.8, 71.3, 46.7, 46.2, 43.3, 34.3, 33.6, 30.5, 29.8, 29.5, 29.0, 25.3, 23.7; ESI-HRMS calcd for $C_{27}H_{27}F_3N_2NaO_4S$ ($M + Na^+$) 555.1536, found 555.1544; HPLC: t_R = 11.80 min, 97.1%. ^{1}H NMR in overall agreement with literature.[12]

***tert*-Butyl (3-(4-(1-(2-(benzo[*b*]thiophen-3-yl)acetyl)-2-methyl-*N*-(4-(trifluoromethyl)-benzyl)azetidine-2-carboxamido)butanamido)propyl)carbamate (7).**

The crude carboxylic acid **2** (40 mg, 75 μmol) in dry DCM (150 μL) was added Et_3N (20 μL, 150 μmol) followed by BOP-Cl (23.9 mg, 94 μmol), and the reaction was heated slowly to 50 °C. After 3 h, additional Et_3N (25 μL, 188 μmol) was added followed by *tert*-butyl (3-aminopropyl)carbamate (17 mg, 1.0 mmol). The reaction was stirred at 50 °C for 30 min, cooled to rt, and stirred over night before concentration *in vacuo* and purification of the crude product by flash chromatography (DCM [5% MeOH]) to yield the desired product as clear sticky oil (23.9 mg, 46%): R_f = 0.12 (DCM [5% MeOH]); ^{1}H NMR (400 MHz, $CDCl_3$) δ 7.93 – 7.51 (m, 4H), 7.49 – 7.13 (m, 5H), 7.24 – 7.11 (m, 1H), 6.79 – 6.40 (m, 1H), 4.92 – 4.49 (m, 2H), 4.47 – 4.27 (m, 1H), 4.24 – 3.84 (m, 3H), 3.78 – 3.38 (m, 2H), 3.26 – 3.16 (m, 2H), 3.14 – 3.00 (m, 2H), 2.58 – 2.41 (m, 1H), 2.38 – 2.20 (m, 1H), 1.94 – 1.73 (m, 5H), 1.71 – 1.48 (m, 4H), 1.43* (s, 9H), 1.42 (s, 9H); ESI-HRMS calcd for $C_{35}H_{43}F_3N_4NaO_5S$ ($M + Na^+$) 711.2798, found 711.2786.

1-(2-(Benzo[*b*]thiophen-3-yl)acetyl)-2-methyl-*N*-(4-((3-((7-nitrobenzo[*c*][1,2,5]oxadiazol-4-yl)amino)propyl)amino)-4-oxobutyl)-*N*-(4-(trifluoromethyl)benzyl)azetidine-2-carboxamide (4).

To a pre-dried microwave vial at rt, the Boc-protected amine **7** (23.9 mg, 35 μmol) was dissolved in dry DCM (70 μL) followed by dropwise addition of TFA (66 μL, 0.867 mmol). Upon full deprotection indicated by TLC the reaction mixture was diluted with DCM, added $NaHCO_3$ (sat), extracted with DCM (x5), the organic phases dried over Na_2SO_4, and

concentrated *in vacuo*. The crude amine (17 mg) was used in the next step without further purification.

To a pre-dried microwave vial under argon were added crude amine (17 mg), NBD-Cl (17.3 mg, 87 μmol), $NaHCO_3$ (9.8 mg, 117 μmol) and the reactants were dissolved in dry MeOH (0.7 mL). The vial was capped, protected from light, and stirred at 50 °C for 4 h. The reaction was cooled to rt, concentrated under N_2 flow, redissolved in EtOAc (2 mL) and water (2 mL), extracted with EtOAc (x3), washed with brine, and concentrated *in vacuo*. The crude product was purified on preparative HPLC using a Phenomenex Luna C18 5 μm column (250×21.20 mm), with gradient elution of 0.05% TFA/MeCN and 0.05% TFA/H_2O at a flow rate of 20 mL/min. HPLC fractions were concentrated under reduced pressure, the remaining aqueous phase extracted with EtOAc (x5), the organic phases washed with brine, and concentrated *in vacuo* to give the desired product as red sticky oil (10.1 mg, 38% over 2 steps): R_f = 0.32 (DCM [10%]); ^{1}H NMR (400 MHz, $CDCl_3$) δ 8.39 (d, J = 8.4 Hz, 1H), 8.01 – 7.92 (m, 1H), 7.84 – 7.77 (m, 1H), 7.72 – 7.67 (m, 1H), 7.63 (d, J = 7.7 Hz, 2H), 7.42 – 7.36 (m, 1H), 7.36 – 7.29 (m, 2H), 7.28 – 7.24 (m, 1H), 7.23 (br s, 1H), 6.01 (d, J = 8.4 Hz, 1H), 4.67 – 4.58 (m, 1H), 4.36 – 4.25 (m, 1H), 4.21 – 3.99 (m, 3H), 3.68 – 3.63 (m, 2H), 3.51 – 3.22 (m, 6H), 2.58 – 2.45 (m, 1H), 2.39 – 2.17 (m, 4H), 1.94 – 1.73 (m, 4H), 1.70 – 1.55 (m, 2H); ESI-HRMS calcd for $C_{36}H_{37}F_3N_7O_6S$ ($M + H^+$) 752.2473, found 752.2502; HPLC: t_R = 12.29 min, 99.9%.

Characterization of excitation and emission properties of 4

Single concentration absorbance and emission spectra of fluorescent tracer **4** was recorded at 8.82 μM. Extinction coefficient for **4** in *n*-octanol was recorded using a FLUOstar Omega Microplate Reader (BMG labtech). Fluorescence spectra for **4** were recorded in duplicates using

a ChronosFD time-resolved spectrofluorometer coupled to PMT detectors. Coumarin 153 (C-153) and **4** were excited at a fixed excitation wavelength of 402 nm, and C-153 in EtOH was used as an internal standard for determination of quantum yield ($\Phi_{C\text{-}153}$ = 0.546 λ_{ex} = 402 nm).[28] All experiments were performed at 25 °C.

IP1 accumulation assay

All IP1 experiments were performed using Flp-In™ T-REx™ 293 cells able to express receptor constructs of interest in an inducible manner. Experiments were carried out using a homogeneous time-resolved FRET-based detection kit (Cis-Bio Bioassays, Codolet, France) according to the manufacturer's protocol. Cells were induced to express the receptor of interest by treatment for 24 h with 100 ng/mL doxycycline and plated at 7500 cells/well in low-volume 384-well plates. The ability of C3 to induce accumulation of IP1 was assessed following a co-incubation for 2 hours with C3, which was preceded by a 15-min pre-incubation with antagonist to allow for equilibration.

Radioligand displacement assay

All receptor radioligand binding experiments using [^{3}H]-**1** were conducted in glass tubes, in binding buffer (50 mM Tris-HCl, 100 mM NaCl, 10 mM $MgCl_2$, 1 mM EDTA, pH 7.4). Membrane protein was generated from Flp-In™ T-REx™ 293 cells induced to express the receptor construct of interest with 100 ng/mL doxycycline. For [^{3}H]-**1** competition binding assays, the radioligand at approximately K_d concentration and varying concentrations of unlabeled ligand of choice were co-added to 5 μg of membrane protein. Non-specific binding of the radioligand was determined in the presence of 10 μM **8**. After an incubation period of 2 h at

25 °C, bound and free [^{3}H]-**1** were separated by rapid vacuum filtration through GF/C glass filters using a 24-well Brandel cell harvester (Alpha Biotech, Glasgow, UK), and unbound radioligand was washed from filters by three washes with ice-cold PBS. After drying (3–12 h), 3 mL of Ultima GoldTM XR (PerkinElmer Life Sciences) was added to each sample vial, and radioactivity was quantified by liquid scintillation spectrometry. Aliquots of [^{3}H]-**1** were also quantified to define the concentration of [^{3}H]-**1** added per tube. Data were fitted to a one-site model using Graphpad Prism v6 and used to calculate pK_i values based on a K_d value for [^{3}H]-**1** of 7.5 nM.[16]

Equilibrium BRET binding assay

The NLuc-hFFA2 construct and cell line were developed as described by Christiansen *et al*.[20] NLuc-hFFA2 Flp-In™ T-REx™ 293 cells were induced to express the receptor construct by treating with 100 ng/mL doxycycline for 24 h. Cells were then harvested and used to make total cell membrane preparations. Membranes were suspended in binding buffer and transferred into a white 96-well plate at 5 μg membrane protein per well. Membranes were then co-incubated with the indicated concentration of **4** (and **1** for non-specific binding measurements; or competing ligand for competition experiments) for 2 h at 30 °C. Following incubation, the NLuc substrate, Nano-Glo (Promega) was added to a final 1:800 dilution. Membranes were incubated a further 5 min before the bioluminescent emission at 460 and 545 nm was measured using a Clariostar plate reader (BMG labtech). Total and non-specific saturation binding data were then globally fit to a one-site binding model using Graphpad Prism v6. Competition binding experiments were fit to a one-site model and used to calculate pK_i values based on a K_d value for **4** of 65.1 nM.

Kinetic BRET binding assay

For kinetic BRET binding assays, cell membranes were generated as for the equilibrium binding assay and again distributed in white 96-well microplates (2.5 μg membrane protein/well). The Nano-Glo substrate was then added (1:800 final dilution) before incubation for 5 min at 30 °C. Plates were then inserted into a Clariostar plate reader, with temperature set to 30 °C and set to read emission at 460 and 545 nm at 90 s intervals. For association experiments **4** (100 nM final concentration) was manually added to the plate after 60 s. Readings were continued at 90 s intervals for the indicated time period. For dissociation experiments the reaction was pre-incubated for 2 h at 30 °C followed by two washes with binding buffer, performed via centrifugation at 14,000 rpm at 4 °C for 15 min. The pellet was then resuspended in binding buffer at 37 °C and transferred into a white 96-well microplate at 90 μL/well and standard kinetic binding assay procedure as described above was followed. In all kinetic experiments parallel wells were assessed in which **1** had been pre-added, and these were used to subtract the non-specific binding signal for **4**. Kinetic binding data were then fit to one-phase association or dissociation models using Graphpad Prism v6 to obtain estimates of k_{off}, k_{on}, and K_d.

Determination of the "On" and "Off" Rates of Unlabeled Ligands through Measurement of Competition Binding Kinetics of 6

The kinetic binding parameters of unlabeled ligands were determined through assessment of the binding kinetics of **4** as described above. Here the standard procedure was followed. After 5 min pre-incubation of membrane protein with Nano-Glo, 6 (100 nM) and three different concentrations of competing unlabeled ligand (1-, 3-, and 10-fold the estimated respective K_i

concentration) were added simultaneously. Readings were then continued at 90 s intervals for 60 min. Three different concentrations of competitor were assessed to ensure that the rate parameters calculated were independent of ligand concentration. Data were fit globally using the kinetics of the competitive binding equation available from GraphPad Prism, with the k_{on} and k_{off} values of **4** entered as constraints.

AUTHOR INFORMATION

Corresponding Author

*Tel: +45 6550 2568. E-mail: ulven@sdu.dk

Author Contributions

The manuscript was written through contributions of all authors. All authors have given approval to the final version of the manuscript. [§]These authors contributed equally.

Funding Sources

The study has been funded by the Danish Council for Strategic Research (grant 11-116196) and the University of Southern Denmark. EC is supported by a fellowship from the Lundbeck Foundation. BDH is supported by a fellowship from the University of Glasgow.

ABBREVIATIONS

BOP-Cl, bis(2-oxo-3-oxazolidinyl)phosphinic chloride; BRET, bioluminescence resonance energy transfer; DHA, docosahexaenoic acid; FFA1, free fatty acid receptor 1 (GPR40); FFA2, free fatty acid receptor 2 (GPR43); FFA3, free fatty acid receptor 2 (GPR41); NBD, 4-nitro-7-aminobenzodiazole; NLUC, NanoLuciferase; PMT, photomultiplier tubes; SS, Stoke's shift.

REFERENCES

(1) Topping, D. L.; Clifton, P. M. Short-chain fatty acids and human colonic function: Roles of resistant starch and nonstarch polysaccharides. *Physiol. Rev.* **2001**, *81*, 1031-1064.

(2) Ulven, T. Short-chain free fatty acid receptors FFA2/GPR43 and FFA3/GPR41 as new potential therapeutic targets. *Front. Endocrinol.* **2012**, *3*, 111.

(3) Milligan, G.; Bolognini, D.; Sergeev, E. *Ligands at the Free Fatty Acid Receptors 2/3 (GPR43/GPR41)*; Springer Berlin Heidelberg: Berlin, Heidelberg, 2016, p 1-16.

(4) Milligan, G.; Shimpukade, B.; Ulven, T.; Hudson, B. D. Complex Pharmacology of Free Fatty Acid Receptors. *Chem. Rev.* **2017**, *117*, 67-110.

(5) Ge, H.; Li, X.; Weiszmann, J.; Wang, P.; Baribault, H.; Chen, J.-L.; Tian, H.; Li, Y. Activation of G Protein-Coupled Receptor 43 in Adipocytes Leads to Inhibition of Lipolysis and Suppression of Plasma Free Fatty Acids. *Endocrinology* **2008**, *149*, 4519-4526.

(6) Tang, C.; Ahmed, K.; Gille, A.; Lu, S.; Grone, H. J.; Tunaru, S.; Offermanns, S. Loss of FFA2 and FFA3 increases insulin secretion and improves glucose tolerance in type 2 diabetes. *Nature Med.* **2015**, *21*, 173-177.

(7) Brown, A. J.; Goldsworthy, S. M.; Barnes, A. A.; Eilert, M. M.; Tcheang, L.; Daniels, D.; Muir, A. I.; Wigglesworth, M. J.; Kinghorn, I.; Fraser, N. J.; Pike, N. B.; Strum, J. C.; Steplewski, K. M.; Murdock, P. R.; Holder, J. C.; Marshall, F. H.; Szekeres, P. G.; Wilson, S.; Ignar, D. M.; Foord, S. M.; Wise, A.; Dowell, S. J. The orphan G protein-coupled receptors GPR41 and GPR43 are activated by propionate and other short chain carboxylic acids. *J. Biol. Chem.* **2003**, *278*, 11312-11319.

(8) Maslowski, K. M.; Vieira, A. T.; Ng, A.; Kranich, J.; Sierro, F.; Yu, D.; Schilter, H. C.; Rolph, M. S.; Mackay, F.; Artis, D.; Xavier, R. J.; Teixeira, M. M.; Mackay, C. R. Regulation of inflammatory responses by gut microbiota and chemoattractant receptor GPR43. *Nature* **2009**, *461*, 1282-1287.

(9) Vinolo, M. A. R.; Ferguson, G. J.; Kulkarni, S.; Damoulakis, G.; Anderson, K.; Bohlooly-Y, M.; Stephens, L.; Hawkins, P. T.; Curi, R. SCFAs Induce Mouse Neutrophil Chemotaxis through the GPR43 Receptor. *Plos One* **2011**, *6*, e21205.

(10) Bjorkman, L.; Martensson, J.; Winther, M.; Gabl, M.; Holdfeldt, A.; Uhrbom, M.; Bylund, J.; Hojgaard Hansen, A.; Pandey, S. K.; Ulven, T.; Forsman, H.; Dahlgren, C. The Neutrophil Response Induced by an Agonist for Free Fatty Acid Receptor 2 (GPR43) Is Primed by Tumor Necrosis Factor Alpha and by Receptor Uncoupling from the Cytoskeleton but Attenuated by Tissue Recruitment. *Mol. Cell. Biol.* **2016**, *36*, 2583-2595.

(11) Forbes, S.; Stafford, S.; Coope, G.; Heffron, H.; Real, K.; Newman, R.; Davenport, R.; Barnes, M.; Grosse, J.; Cox, H. Selective FFA2 Agonism Appears to Act via Intestinal PYY to Reduce Transit and Food Intake but Does Not Improve Glucose Tolerance in Mouse Models. *Diabetes* **2015**, *64*, 3763-3771.

(12) Pizzonero, M.; Dupont, S.; Babel, M.; Beaumont, S.; Bienvenu, N.; Blanque, R.; Cherel, L.; Christophe, T.; Crescenzi, B.; De Lemos, E.; Delerive, P.; Deprez, P.; De Vos, S.; Djata, F.; Fletcher, S.; Kopiejewski, S.; L'Ebraly, C.; Lefrancois, J. M.; Lavazais, S.; Manioc, M.; Nelles, L.; Oste, L.; Polancec, D.; Quenehen, V.; Soulas, F.; Triballeau, N.;

van der Aar, E. M.; Vandeghinste, N.; Wakselman, E.; Brys, R.; Saniere, L. Discovery and Optimization of an Azetidine Chemical Series As a Free Fatty Acid Receptor 2 (FFA2) Antagonist: From Hit to Clinic. *J. Med. Chem.* **2014**, *57*, 10044-10057.

(13) Ang, Z.; Ding, J. L. GPR41 and GPR43 in Obesity and Inflammation - Protective or Causative? *Front Immunol* **2016**, *7*, 28.

(14) Kimura, I.; Ozawa, K.; Inoue, D.; Imamura, T.; Kimura, K.; Maeda, T.; Terasawa, K.; Kashihara, D.; Hirano, K.; Tani, T.; Takahashi, T.; Miyauchi, S.; Shioi, G.; Inoue, H.; Tsujimoto, G. The gut microbiota suppresses insulin-mediated fat accumulation via the short-chain fatty acid receptor GPR43. *Nature Commun.* **2013**, *4*, 1829.

(15) Namour, F.; Galien, R.; Van Kaem, T.; Van der Aa, A.; Vanhoutte, F.; Beetens, J.; Van't Klooster, G. Safety, pharmacokinetics and pharmacodynamics of GLPG0974, a potent and selective FFA2 antagonist, in healthy male subjects. *Br. J. Clin. Pharmacol.* **2016**, *82*, 139-148.

(16) Vermeire, S.; Kojecký, V.; Knoflícek, V.; Reinisch, W.; Kaem, T. V.; Namour, F.; Beetens, J.; Vanhoutte, F. GLPG0974, an FFA2 antagonist, in ulcerative colitis: efficacy and safety in a multicenter proof-of-concept study. *J Crohns Colitis* **2015**, *Suppl 1*, S39.

(17) Ma, Z.; Du, L.; Li, M. Toward Fluorescent Probes for G-Protein-Coupled Receptors (GPCRs). *J. Med. Chem.* **2014**, *57*, 8187-8203.

(18) Christiansen, E.; Hudson, B. D.; Hansen, A. H.; Milligan, G.; Ulven, T. Development and Characterization of a Potent Free Fatty Acid Receptor 1 (FFA1) Fluorescent Tracer. *J. Med. Chem.* **2016**, *59*, 4849-4858.

(19) Yates, A. S.; Doughty, S. W.; Kendall, D. A.; Kellam, B. Chemical modification of the naphthoyl 3-position of JWH-015: in search of a fluorescent probe to the cannabinoid CB2 receptor. *Bioorg. Med. Chem. Lett.* **2005**, *15*, 3758-3762.

(20) Petrov, R. R.; Ferrini, M. E.; Jaffar, Z.; Thompson, C. M.; Roberts, K.; Diaz, P. Design and evaluation of a novel fluorescent CB2 ligand as probe for receptor visualization in immune cells. *Bioorg. Med. Chem. Lett.* **2011**, *21*, 5859-5862.

(21) Toyo'oka, T.; Watanabe, Y.; Imai, K. Reaction of amines of biological importance with 4-fluoro-7-nitrobenzo-2-oxa-1,3-diazole. *Anal. Chim. Acta* **1983**, *149*, 305-312.

(22) Lin, S.; Struve, W. S. Time-resolved fluorescence of nitrobenzoxadiazole-aminohexanoic acid: effect of intermolecular hydrogen-bonding on non-radiative decay. *Photochem. Photobiol.* **1991**, *54*, 361-365.

(23) Stoddart, L. A.; Johnstone, E. K.; Wheal, A. J.; Goulding, J.; Robers, M. B.; Machleidt, T.; Wood, K. V.; Hill, S. J.; Pfleger, K. D. Application of BRET to monitor ligand binding to GPCRs. *Nat. Methods* **2015**, *12*, 661-663.

(24) Sergeev, E.; Hansen, A. H.; Pandey, S. K.; MacKenzie, A. E.; Hudson, B. D.; Ulven, T.; Milligan, G. Non-equivalence of Key Positively Charged Residues of the Free Fatty Acid 2 Receptor in the Recognition and Function of Agonist Versus Antagonist Ligands. *J. Biol. Chem.* **2016**, *291*, 303-317.

(25) Tikhonova, I.; Poerio, E. Free fatty acid receptors: structural models and elucidation of ligand binding interactions. *BMC Structural Biology* **2015**, *15*, 16.

(26) Brantis, C. E.; Ooms, F.; Bernard, J. Novel amino acid derivatives and their use as GPR43 receptor modulators. *PCT Int. Appl. WO2011092284* **2011**.

(27) Hudson, B. D.; Tikhonova, I. G.; Pandey, S. K.; Ulven, T.; Milligan, G. Extracellular Ionic Locks Determine Variation in Constitutive Activity and Ligand Potency between

Species Orthologs of the Free Fatty Acid Receptors FFA2 and FFA3. *J. Biol. Chem.* **2012**, *287*, 41195-41209.

(28) Rurack, K.; Spieles, M. Fluorescence quantum yields of a series of red and near-infrared dyes emitting at 600-1000 nm. *Anal. Chem.* **2011**, *83*, 1232-1242.

TABLE OF CONTENT GRAPHICS